Lateral Transport in Two-dimensional Heterojunction Interlayer Tunneling Field Effect Transistor (Thin-TFET)

Mingda (Oscar) Li[1], David Esseni[2], Debdeep Jena[1], Huili Grace Xing[1]
[1]University of Notre Dame, IN 46556, USA. [2]University of Udine, Udine 33100, Italy
Tel: 1-574-631-9108, Fax: 1-574-631-4393, Email: hxing@nd.edu, mli7@nd.edu

The single particle model has been developed for the tunneling between two monolayer two-dimensional (2D) semiconductors [1]. Based on this model, a novel Two-dimensional Heterojunction Interlayer Tunneling Field Effect Transistor (Thin-TFET) (see **Fig.1a**) is proposed to achieve very steep subthreshold swing [1]. However, the initial study ignored the lateral transport in the top and bottom 2D layers. In this work, we study the effect of the lateral transport on the on-current area density and the sub-threshold swing (SS) of the Thin-TFET.

The current flow in the Thin-TFET is illustrated in **Fig.1b**. Current continuity equations in both the top and bottom layers are written as **Eq.1a** and **Eq.1b**, where $J^{T(B)}_{Drift(Diff.)}(x)$ is the drift (diffusion) current density in the top (bottom) layer at the point x, $J_T(x)$ is the vertical tunnel current at the point x. To achieve a good electrostatic control, we designed the Thin-TFET such as the top layer semiconductor is non-degenerate n-type while the bottom layer is degenerate p-type [1]. Thus, the sum of the drift and diffusion currents in both top and bottom 2D layers are shown in **Eq.2a** and **Eq.2b** [2], where $n^{2D}_T(x)$ and $p^{2D}_B(x)$ are the 2D electron concentration in the top layer and 2D hole concentration in the bottom layer at the point x, $E_{FT(B)}$ is the electron (hole) quasi-Fermi level in the top (bottom) layer. $\mu_{T(B)}$ is the electron (hole) mobility in the top (bottom) 2D layer, D_B and $\mathcal{E}$ are the hole diffusivity and lateral electrical field in the bottom 2D layer respectively. To further simplify the equation, we introduction the Fermi potential in the top (bottom) layer: $V_{FT(B)} = -E_{FT(B)}/e$, where e is the electron charge. Therefore, the potential in the bottom layer can be expressed as $V_B = V_{FB} - \phi_B$, where $\phi_B = (E_{FB} - E_{VB})/e$. E_{VB} is the valence band edge of the bottom 2D layer. Considering $\mathcal{E} = -V_B/e$ and combining **Eq.1a-b** and **Eq.2a-b**, we get two differential equations **Eq.3a** and **Eq.3b**, with the corresponding boundary conditions listed in **Eq.4a-d**.

In **Eq.3a-b**, $n^{2D}_T(x)$, $p^{2D}_B(x)$, $\phi_B(x)$, and $J_T(x)$ are determined by the local top gate voltage $V_{TG,L}(x)$= V_{TG} - $V_{FB}(x)$, local back gate voltage $V_{BG,L}(x)$ =V_{BG} -$V_{FB}(x)$ and local Fermi potential difference $V_{TB,L}(x)$ =$V_{FT}(x)$-$V_{FB}(x)$ through the model explained in [1], where $V_{T(B)G}$ are the applied top (back) gate voltage. $J_T(x)$, $n^{2D}_T(x)$, $p^{2D}_B(x)$, and $\phi_B(x)$ are solved self-consistently with the differential equations **Eq.3a-b** using the Newton's method with Hessian modification along with the backtracking line search [3]. The absolute error of $\partial^2 V_{FT(B)}(x)/\partial x^2$ is converged to be less than 0.00375 V/nm^2.

The material system and modeling parameters are listed in **Fig.1c**. The top oxide and back oxide have the effective oxide thickness of 1 nm. The interlayer thickness is 0.6 nm. The lead resistors R_{LT} and R_{LB} are ignored. **Figure 2a** shows the J_D-V_{TG} and J_D-V_{DS} curves without considering the lateral transport. The average SS is extract in the J_T range from 10^{-4} to 10^{-1} $\mu A/\mu m^2$ (10^{-6} to 10^{-3} A/m in **Fig.2b**). The Fermi potential distribution in the top 2D layers (V_{FT}) with different gate lengths as shown in **Fig.2b**. The V_{FT} increases along x-direction due to the lateral transport effects and reaches the drain voltage (0.3 V) at the drain end. Since the top layer is non-dengenrate while the bottom layer is degenerate, most of the potential drop in the top layer. As expected, the insert figure of **Fig.2b** shows the change of V_{FB} is much smaller than change of V_{FT}. Although the lateral transport affects the Fermi potential in the top and bottom 2D layers, the on-current area density and the subthreshold slope remain intact according to **Fig.2c**. Below is the explanation: the drain current is the sum of $J_T(x)$, $J_T(x)$ is determined by $V_{TG,L}(x)$, $V_{BG,L}(x)$, and $V_{DS,L}(x)$. Along x-direciton, only $V_{DS,L}(x)$ is changing significantly from 0.3 V to ∼0.2 V. According to the J_D-V_{DS} curve in **Fig.2a**, $J_T(x)$ remain almost the same when V_{DS} ranging from 0.2 V to 0.3 V. Thus the total current area density remain almost the same even with the lateral transport effect.

To summarize, we develop the lateral transport model for the proposed Thin-TFET. It shows that when the top layer and bottom layer 2D materials has the mobility of 100 cm^2/Vs and the diffusivity of 5 cm^2/s, the lateral transport will not deteriorate either the on-current or the sub-threshold slope of the Thin-TFET. Further studies are required to find out the minimum requirements of mobility and diffusivity in the top and bottom 2D layer, as well as investigate the effect of the lead region resistances.

Acknowledgments: This work was supported by the Center for Low Energy Systems Technology (LEAST).

References

[**1**] M.Li *et al. J. of Applied Physics*, **115**, 074508 (2014). [**2**] S.M.Sze *et al. John Wiley & Sons*, (2006).
[**3**] J.Nocedal *et al. Springer-Verlag*, (2006).

$$-\partial\left[J^T_{Drift}(x)+J^T_{Diff.}(x)\right]/\partial x - J_T(x) = 0 \quad \textbf{(1a)} \qquad -\partial\left[J^B_{Drift}(x)+J^B_{Diff.}(x)\right]/\partial x + J_T(x) = 0 \quad \textbf{(1b)}$$

$$J^T_{Drift}(x)+J^T_{Diff.}(x) = \mu_T n^{2D}_T(x)\partial E_{FT}/\partial x \quad \textbf{(2a)}$$

$$J^B_{Drift}(x)+J^B_{Diff.}(x) = \mu_B p^{2D}_B(x)\mathcal{E} - eD_B\partial p^{2D}_B(x)/\partial x \quad \textbf{(2b)}$$

$$\partial^2 V_{FT}(x)/\partial x^2 = J_T(x)/en^{2D}_T(x)\mu_T \quad \textbf{(3a)}$$

$$\partial^2\left[V_{FB}(x)-\phi_B(x)\right]/\partial x^2 + \left[D_B/p^{2D}_B(x)\mu_B\right]\partial^2 p^{2D}_B(x)\partial x^2 = -J_T(x)/ep^{3D}_B(x)\mu_B \quad \textbf{(3b)}$$

$$V_{FT}(L) = V_{DS} \quad \textbf{(4a)} \qquad V_{FB}(0) = 0 \quad \textbf{(4b)}$$

$$J^T_{Drift}(0)+J^T_{Diff.}(0) = 0 \quad \textbf{(4c)} \qquad J^B_{Drift}(L)+J^B_{Diff.}(L) = 0 \quad \textbf{(4d)}$$

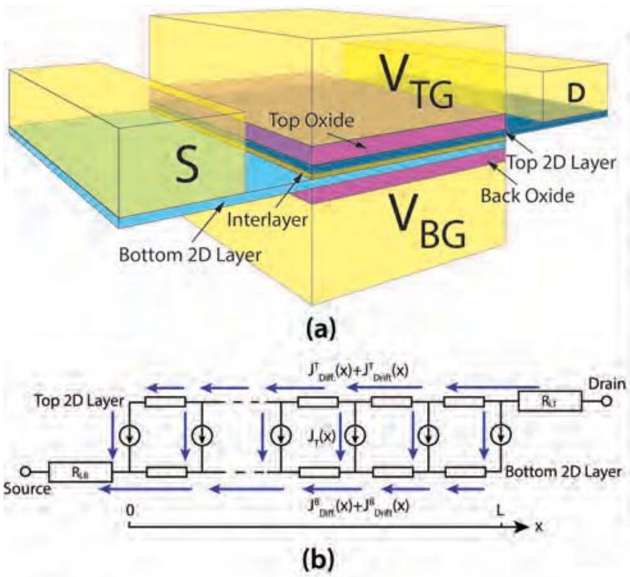

Material system for n-type Thin-TFET				
Gate metal workfunctions: $\Phi_{M,T} = 4.06\ eV$, $\Phi_{M,B} = 5.25\ eV$				
	Bandgap (eV)	Electron affinity (χ) (eV)	m^*_c (m_0)	m^*_v (m_0)
MoS_2	1.6	4.25	0.378	0.461
WTe_2	0.9	3.65	0.235	0.319

Modeling parameters for vertical tunneling [1]	
Matrix Element M_{B0} (eV)	0.01
Scattering correlation length L_C (nm)	10
Wave-function decay constant in the interlayer κ (nm^{-1})	3.8
Energy broadening σ (meV)	10

Modeling parameters for lateral tranport	
Mobility in the top(bottom) 2D layer $\mu_{T(B)}$ (cm^2/Vs)	100
Diffusivity in the top(bottom) 2D layer $D_{T(B)}$ (cm^2/s)	5

Figure 1: (a) Schematic structure of the Thin-TFET; (b) the sketch of the current flow in the Thin-TFET, define the lateral direction of the Thin-TFET as x-direction; (c) the material system and the modeling parameters.

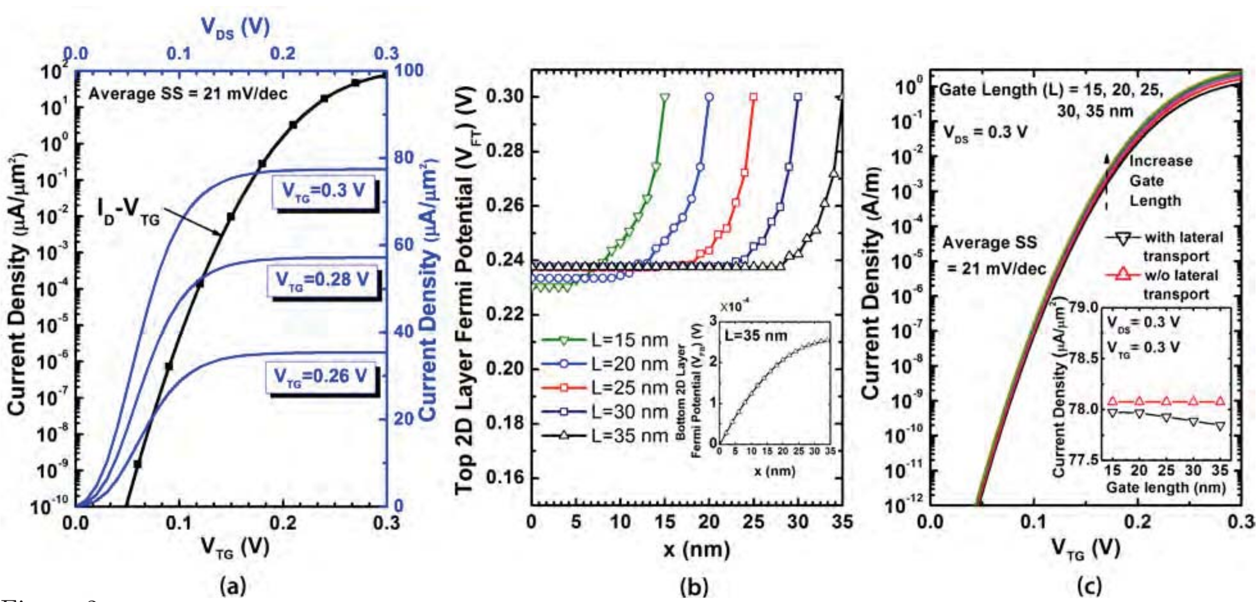

Figure 2: (a) The J_D-V_{TG} curve at $V_{DS} = 0.3$ V and J_D-V_{DS} curve without lateral transport; (b) the top 2D layer Fermi potential at different positions along x-direction with different gate lengths, the insert figure show the bottom 2D layer Fermi potential at different position along x-direction with gate length of 35 nm; (c) the I_D-V_{TG} curves with different gate lengths with lateral transport, the insert figure shows the J_D versus gate length at $V_{TG} = 0.3$ V with and without lateral transport.